Contents list available at CBIORE journal website

International Journal of Renewable Energy Development

Journal homepage: https://ijred.cbiore.id

Research Article

CFD analysis of photovoltaic panel performance under variable weather conditions with natural and forced convective cooling

Ayaz Aydin Abduljabbar[1*], Manar Mohammed[2], Zahraa H. Mohammed Ali[3], Hussein Hayder Mohammed Ali[2], Furqan Haider Mohammed Ali[2], Timur Choban Khidir[1]

[1]*Mechanical Engineering Department, College of Engineering, University of Kirkuk, Kirkuk 36001, Iraq*

[2]*Department of Mechanical Power Techniques Engineering, Technical College Engineering- Kirkuk, Northern Technical University, Kirkuk 36001, Iraq*

[3]*Chemical Industry Technologies Department, Kirkuk Polytechnic College, Northern Technical University, Kirkuk 36001, Iraq*

Abstract. The objective of this study is to numerically investigate the influence of climatic conditions, particularly ambient temperature and relative humidity, on the thermal and electrical performance of photovoltaic (PV) panels, and to evaluate the effectiveness of natural and forced convection cooling for both conventional and finned panel configurations. A multilevel computational fluid dynamics (CFD) model was developed using ANSYS Fluent 16.1 under realistic environmental conditions of Baghdad, Iraq. Two configurations were examined: a conventional flat panel and a modified panel equipped with longitudinal fins acting as a passive heat sink. Under both natural and forced convection, with an inlet air velocity of 1.5 m/s for forced cooling, the simulations took into account solar radiation, species transport to capture humidity effects, and the k–ω turbulence model. Under natural convection, the traditional panel attained a maximum surface temperature of 333.11 K with an electrical efficiency of 27.8%; forced convection lowered the temperature to 319.22 K and increased efficiency to 29.88% (7.5% improvement). Under natural cooling, the finned design lowered the temperature to 327.4 K, raising the efficiency to 28.66% (~3% increase). Under forced cooling, it further dropped to 315.5 K, reaching a maximum efficiency of 30.43%. This translates to advancements of 9.4% over the traditional natural cooling scenario and 6.17% over the finned natural cooling scenario. Yearly average results show that the finned design improves electrical efficiency by about 2% under natural convection and up to 6.53% under forced convection, whereas forced cooling of the conventional panel gives a 3.12% increase. The enhancement is primarily attributed to increased heat transfer surface area and improved convective mixing, particularly under natural convection where fin-induced vortices significantly enhance heat dissipation.

Keywords: Solar energy, Photovoltaic, fins, computational fluid dynamics, Thermodynamic analysis, finite volume method

Received: 6th Feb 2026; Revised: 27th April 2026; Accepted: 15th May 2026; Available online: 21st May 2026

1. Introduction

Among the most often used renewable energy sources were solar panels, which were vital for providing power for commercial establishments, industrial plants, and homes. Many uses embraced them because of their simplicity of installation, low manufacturing cost, and minimal carbon emissions (Raza *et al.* 2026; Sheikh *et al.* 2024; Nematpour Keshteli *et al.* 2024). These panels were made mostly of silicon; environmental factors drastically influenced their electrical efficiency as their electrical performance fell when photovoltaic cells were exposed to strong solar radiation and high temperatures. Efficiency fell by around 0.4-0.5% for every one-degree Celsius over the operating temperature. Because of photovoltaic systems' great thermal sensitivity, effective thermal management was essential for improving electrical performance, guaranteeing dependability, and prolonging operational lifetime. Lowering panel temperature via cooling systems relying on natural or forced convection improves efficiency, therefore reducing thermal stresses and avoiding hotspot formation. By simulating the consequences of solar radiation, ambient temperature, wind speed, and convective heat transfer on panel temperature, therefore investigating the thermal behavior of solar panels, numerical modeling was used to evaluate the efficiency of different cooling systems.

The ambient air temperature was found to be among the most crucial variables affecting solar panel performance. Solar cell temperature increased along with air temperature thanks to solar absorption and limited convective heat dissipation (Seto *et al.* 2024; Khodadadi & Sheikholeslami 2022). With cell temperature increasing, the semiconductor voltage fell, therefore lowering electrical efficiency by roughly 0.4-0.5% per degree Celsius in most silicon-based panels. Under warm surrounding conditions, heat losses also rose, therefore increasing the probability of long-term material deterioration and hotspot creation. High temperatures in tropical and desert areas lowered panel production notwithstanding strong solar illumination levels. Natural or forced cooling techniques decreased cell temperature, increased efficiency, and extended panel life (Hossam *et al.* 2025; Shrivastava *et al.* 2022; Omri *et al.* 2022).

* Corresponding author
Email: ayaz.hurmuzi@uokirkuk.edu.iq (A.A. Abduljabbar)

https://doi.org/10.61435/ijred.2026.62339
ISSN: 2252-4940/© 2026.The Author(s). Published by CBIORE

Directly and indirectly via optical, thermal, and physical processes, temperature and relative humidity influenced the electrical behavior of solar cells. Increased air water vapor content from high humidity led to more scattering and refraction of solar radiation, therefore lowering the absorbed energy (Zarda *et al.* 2022). High humidity did marginally improve convective heat transfer by boosting air density, yet this impact was small in relation to ambient temperature (Qader *et al.* 2023). High humidity also sped corrosion at metallic joints and encouraged condensation under the glass layer. Studies using MATLAB showed that lower voltage and current outputs resulted from water molecules reflecting solar radiation and lowering absorbed energy (Kumar & Subbarao 2025; Bekbolatova *et al.* 2025; Sun *et al.* 2023; Wen *et al.* 2025; Akpinar *et al.* 2025). Experimental measurements of voltage and current at various humidity levels revealed that raising humidity reduces power production. Tripathi *et al.* (2021) experimentally showed that a little drop in surface temperature and reduced panel efficiency resulted from higher relative humidity. Under different temperature and humidity levels, Sardouei *et al.* (2018) investigated the thermal and electrical performance of different photovoltaic-thermal (PVT) water collector designs using a combined 3D computational fluid dynamics (CFD) simulation and experimental validation approach. The study shows that spiral flow heat exchanger designs provide the most uniform temperature distribution and high electrical efficiency, while direct flow designs create localized hot zones on the PV module surface. The use of cross-fins in box-type collectors significantly reduces hot zones and improves performance.

Hasan *et al.* (2022) tested a 120 Wp panel in Nasiriyah city experimentally assessing the effects of clouds, rain, humidity, and wind speed and confirmed that higher humidity negatively impacted voltage, current, and electric power output; wind speed increased electrical performance by lowering panel temperature; clouds and rain lowered solar radiation intensity; hence significantly reduced power generation. Zarda *et al.* (2023) reviewed the application of nanofluids in flat-plate solar collectors and demonstrated that nano-particle dispersion significantly improves thermal conductivity, convective heat transfer, and system efficiency, while also identifying practical limitations related to increased pressure drop and pumping power, thereby providing guidance for future experimental optimization of solar water heating systems. Higher humidity and temperature conditions have also been linked to increased leakage currents and insulation degradation. Highlighting the need of cooling solutions, Hassan *et al.* (2022) showed that panel efficiency drops dramatically at high temperatures. Acheme (2025) declared that electrical output was greater under moderate temperatures and declined by around 0.3-0.5% per degree Celsius over standard circumstances. Sepulveda 2025 focused on the long-term effects of humidity on solar panel materials and their components, demonstrating that high humidity accelerates corrosion and PID (Potential Induced Degradation), and can cause a decrease in nominal current and voltage over time of up to 7% and 0.66%, respectively. Homa *et al.* (2024) experimentally and numerically studied an active air-cooling system for PV panels under 770 W/m² irradiance. The power output of a 70 Wp panel decreased from 47.31 W to 40.09 W at 60°C, while the cooled system improved it to 44.37 W (10.7% increase). Using commercial solver based on finite volume method, an optimal fan orientation of 7° vertical and 10° horizontal tilt was identified, yielding a net power gain of about 3.1% after accounting for fan energy consumption. The objective of this research work is to numerically investigate the influence of climatic conditions, particularly ambient temperature and relative humidity, on the thermal and electrical performance of PV panels using ANSYS Fluent commercial solver. The study intends to evaluate and compare the effectiveness of natural and forced convection cooling methods for two panel arrangements: a standard flat panel and a finned panel with a passive heat-sink design under the real-world environmental circumstances of Baghdad, Iraq. Additionally, the study seeks to evaluate the increase in electrical efficiency and heat dissipation obtained by fin integration, as well as to examine air flow patterns and temperature distribution over an annual cycle.

2. Methodology

2.1 System and model description

Using both natural and forced convection techniques under operating conditions imitating the surrounding ambient environment including relative humidity and mean temperatures over an annual cycle the effect of cooling on a solar panel subjected to direct sunlight was studied here. The study looked at the representative average day of each month, which is frequently used in solar system performance analyses. For a site in Baghdad (longitude 49.36°, latitude 33.31°) at 12:00 PM on the average solar day of each month throughout the year, the numerical analysis was carried out. Relative humidity is shown in Figure 1 along with the highest, smallest, and average temperatures for these days. Two solar panel designs were investigated: a basic panel and a altered panel fitted with a heat sink under the surface. Both models were examined under natural and forced convection cooling settings (Hasan *et al.* 2022).

2.2 Software setup

The geometric configurations of the conventional PV panel (Case 1) panel without any geometric modification was considered as the baseline configuration. Heat dissipation from the panel occurs through convection and radiation over a smooth rear surface, without any enhancement features. This case was intended to illustrate in practice how PV systems operate. Under the identical setting of the boundary the simulation were conducted for example the solar radiation intensity, ambient temperature and relative humidity.Both natural and forced convection modes was investigated to obtain how airflow affects panel temperature and electrical efficiency. The new PV panels (Case 2) have fins along the back that act as passive cooling systems to help heat disperse. Due to adding

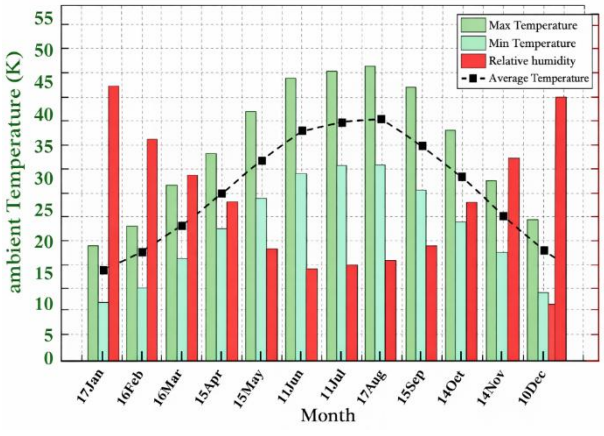

Fig. 1 Monthly relative humidity and ambient temperature (maximum, minimum, and average) for the representative solar day.

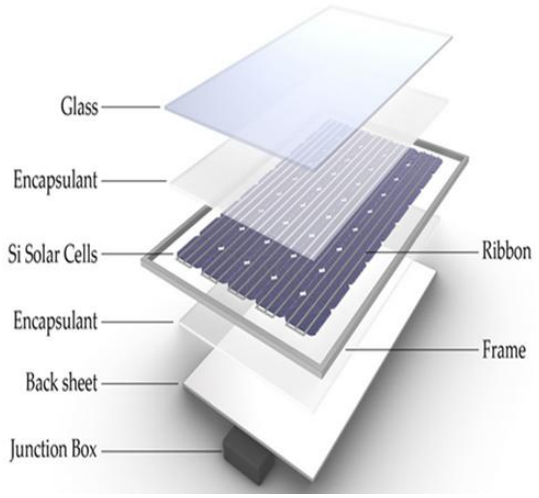

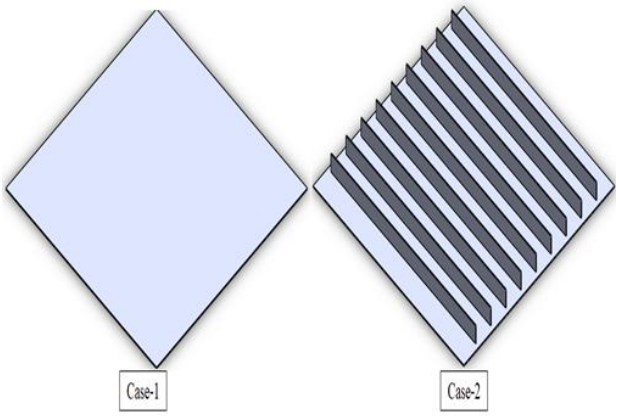

Fig. 2 a) The components of solar panel, **b)** 3D view of the geometric models of the conventional PV panel and the finned panel with heat-sink structure.

fins the effective heat transfer area is increased and improves convective heat transmission, especially under natural convection where buoyancy driven flow is extensive. Similar to Case 1, simulations were carried out under the same environmental and operating conditions to guarantee a consistent comparison, as shown in Figure 2(a,b). The panel had a square form and measured 0.5 metres by 0.5 metres. In the design two, longitudinal fins were added all along the panel's underside to serve as a passive heat sink. Every fin had a thickness of 2 mm and a height of 25 mm, therefore increasing the surface area available for convective heat transmission. The construction consisted of a top glass cover, an anti-reflective coating (ARC), ethylene-vinyl acetate (EVA) encapsulation layers, silicon PV cells, and an aluminium supporting back plate. These layers were developed to simulate the optical and thermal performance of a normal PV module. The surrounding domain consisted of ambient air containing water vapor to represent relative humidity effects. The thermophysical properties of all solid materials and the air-water vapor mixture were defined according to the values presented in Table 1, including density, specific heat capacity, thermal conductivity, viscosity, and layer thickness. This material definition enabled accurate simulation of heat conduction within the panel layers and convective heat transfer between the panel surfaces and the surrounding humid air. The panel was surrounded by humid ambient air containing water vapor due to relative humidity effects. The thermophysical properties of the panel materials and the surrounding air–vapor mixture are presented in Table 1 (Ali *et al.* 2023; Mohamad 2024; Ali *et al.* 2024; Abbass & Abduljabbar 2022).

3. Mathematical model

3.1 Governing equations

The mathematical model under consideration consists of a set of governing equations, namely the continuity, conservation of momentum, energy, and turbulence equations for the fluid, whereas for the solid plate, only the energy equation is solved by conduction. The fluid under consideration, a mixture of air and water vapor (representing the moisture content), is considered an ideal incompressible fluid; that is, density changes are calculated from temperature changes, with pressure changes being neglected. For the fluid, which is a mixture of air and vapor, the governing equations are (Ali *et al.* 2024; Qader *et al.* 2024; Berkache *et al.* 2024):

(a) Continuity Equation (Conservation of Mass):

$$\frac{\partial \boldsymbol{\rho}}{\partial \mathbf{t}} + \boldsymbol{\nabla} \cdot (\boldsymbol{\rho}\mathbf{u}) = \mathbf{0} \qquad (1)$$

In these equations, $\boldsymbol{\rho}$ denotes the fluid density, $\mathbf{t}$ represents time, $\mathbf{u}$ is the velocity vector, and $\boldsymbol{\nabla}$ denotes the divergence operator.

(b) Momentum Equation (Navier-Stokes Equation):

$$\boldsymbol{\rho}\left(\frac{\partial \mathbf{u}}{\partial \mathbf{t}} + (\mathbf{u} \cdot \boldsymbol{\nabla})\mathbf{u}\right) = -\boldsymbol{\nabla}\mathbf{p} + \boldsymbol{\mu}\boldsymbol{\nabla}^{\mathbf{2}}\mathbf{u} + \mathbf{f} \qquad (2)$$

Where $\mathbf{p}$ denotes the pressure, $\boldsymbol{\mu}$ represents the dynamic viscosity of the fluid, $\boldsymbol{\nabla}^{\mathbf{2}}$is the Laplacian operator corresponding to a second-order spatial differential, and $\mathbf{f}$ denotes the external force vector acting per unit volume.

(c) Energy Equation:

For fluid zone

$$\boldsymbol{\rho}\left(\frac{\partial \mathbf{E}}{\partial \mathbf{t}} + \mathbf{u} \cdot \boldsymbol{\nabla}\mathbf{E}\right) = -\boldsymbol{\nabla} \cdot \big(\mathbf{u}(\mathbf{p} + \mathbf{E})\big) + \boldsymbol{\nabla} \cdot (\boldsymbol{\kappa}\boldsymbol{\nabla}\mathbf{T}) + \boldsymbol{\Phi} \qquad (3)$$

Table 1
The physical properties of the materials used and the surrounding ambient air

Propertiese	water	Water vapor	encapsulant	PV-Cell	Glass	Aluminum
Density Kg/m^3	998.2	0.5542	960	2330	3000	2719
Specific heat J/Kg. k	4186	2014	2090	677	500	871
Thermal conductivity W/m. K	0.6	0.0261	0.35	148	1.8	202.4
Viscosity Pa.sec	0.001003	1.34×10^{-5}	--	---	--	--
Thickness m	----	-----	1×10^{-5}	2×10^{-4}	0.003	0.002

In this equation, **E** denotes the internal energy, **κ** represents the thermal conductivity, **T** is the temperature, and **Φ** denotes the dissipation function. To characterize heat transfer through a solid, drawing each layer of the sheet as an independent solid zone with such small thicknesses would generate a poor mesh in these layers, negatively impacting the solution. Therefore, it can be represented using shell-conduction in the software, which solves the two-dimensional heat transfer equation for conduction through these layers. The equation for thermal conduction through solid layers is given by (Qader 2024; Miri *et al.* 2023):

$$\nabla \cdot (K_w \nabla T_w) = 0 \quad (4)$$

Where $K_w$represents the thermal conductivity of the wall material, while T_w represents the surface temperature of the wall.

3.2 k-omega Turbulence Model

(a) Turbulent Kinetic Energy (**k**) Equation: Describes the energy contained in turbulence (Mohanty *et al.* 2024; Zina Abd Alameer Al Shadidi 2020).

$$\frac{\partial k}{\partial t} + u_j \frac{\partial k}{\partial x_j} = \frac{\partial}{\partial x_j}\left[\left(\nu + \frac{\nu_t}{\sigma_k}\right)\frac{\partial k}{\partial x_j}\right] + P_k - \beta^* k\omega \quad (5)$$

The term **ν** denotes the kinematic viscosity, $\nu_t$represents the turbulent viscosity, σ_k and σ_ω are the Prandtl numbers associated with **k** and **ω**, respectively, P_k is the turbulent production term, and **α**, **β**, and $\beta^*$are model constants.

(b) Specific Dissipation Rate (**ω**) Equation: Represents the rate of dissipation of turbulent kinetic energy per unit energy (Avithi *et al.* 2015; Barrak *et al.* 2022).

$$\frac{\partial \omega}{\partial t} + u_j \frac{\partial \omega}{\partial x_j} = \frac{\partial}{\partial x_j}\left[\left(\nu + \frac{\nu_t}{\sigma_\omega}\right)\frac{\partial \omega}{\partial x_j}\right] + \alpha \frac{\omega}{k} P_k - \beta \omega^2 \quad (6)$$

(c) Species transport equation

In order to represent humidity and its effect on the study, the species transport equation, which represents multispecies problems, must be used (Manar *et al.* 2025; Ali & Ahmed 2024).

$$\frac{\partial \rho Y_i}{\partial t} + \nabla(\rho \vec{v} Y_i) = -\nabla(J_i) + R_i + S_i \quad (7)$$

Where R_i represents the rate of production of type i of concentration Y_i from chemical reactions, and S_i is the rate of generation of type i of concentration Y_i from an internal source, while J_i represents the diffusion flux of type i and is given by the relation:

$$J_i = -\rho D_{m,i} \nabla(Y_i) - D_{T,i} \frac{\nabla T}{T} \quad (8)$$

Where $D_{m,i}$ is the mass-diffusion coefficient and $D_{T,i}$ is the thermal-diffusion coefficient. The value 2.88×10^{-5} m²/sec was used for the mass-diffusivity.

Solar radiation was applied to the panel using a solar model that uses a specific algorithm within Fluent in order to shade the surfaces exposed to solar radiation and convert this energy into an internal energy source within the cells according to the intensity of their exposure to solar radiation. The electrical efficiency of PV panel, as a function of cell temperature T_c, is obtained by the following equation.

$$\eta_{el} = \eta_{ref}(1 - 0.0045(T_c - 298.15)) \quad (9)$$

Where η_{ref} The solar panel's efficiency is represented at a reference temperature, which is approximately 33% at this temperature (Ali *et al.* 2025).

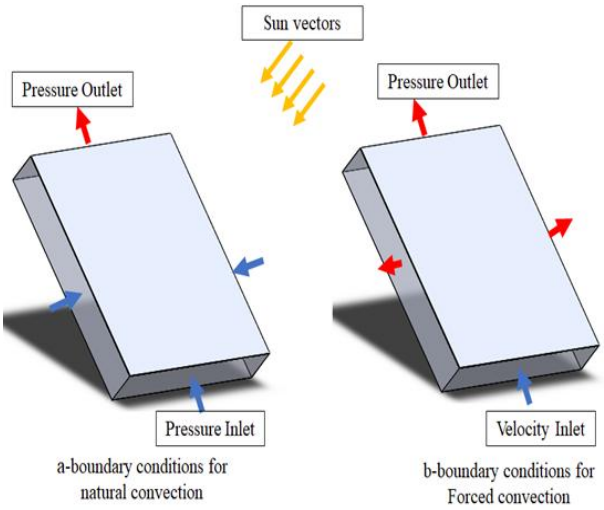

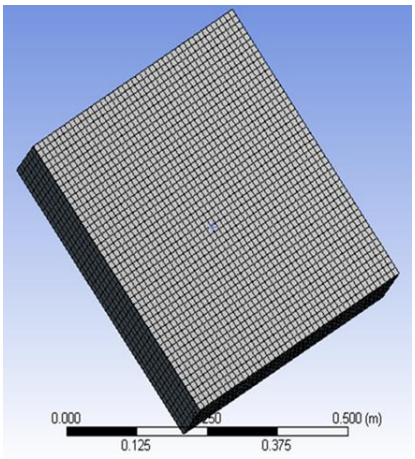

Fig. 3 a) Zone selection and boundary conditions, **b)** Structural mesh generated

3.3 Boundary conditions

For the inlet and outlet boundaries, the inlet temperature is prescribed based on the average ambient temperature, while the humidity is specified as the mass fraction of water vapor according to the values shown in Figure 1. Forced cooling is modeled by imposing an inlet airflow velocity of 1.5 m/s. In this study, a consistent geometric mesh was generated for all investigated models, maintaining the same number of cells and growth rate. The mesh consists of structured hexahedral elements, providing an ordered and uniform discretization of the computational domain, as shown in Figure 3(a,b). This configuration ensures high numerical accuracy and stability in simulating fluid flow and heat transfer due to its low numerical diffusion and high element quality.

3.4 Computational domain and grid details

A mesh independence analysis demonstrated that the solution becomes stable at approximately 700,000 cells, which was therefore adopted for all simulations. Additionally, the mesh is refined in regions near the panel surfaces and fins to accurately capture temperature gradients and boundary layer behavior,

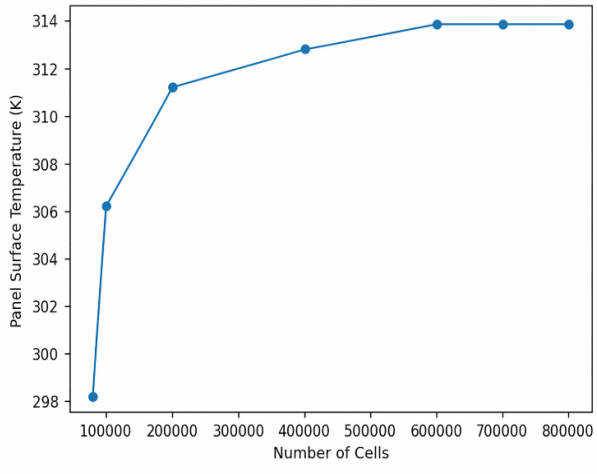

Fig. 4 Mesh independence study

while a gradual growth rate is applied toward the outer domain to minimize computational cost.

In order to study the solution's mesh independence, the panel surface temperature value of the Solar panel was taken for the case 1 under natural convection 12:00 on the day of 14/ at a different number of cells. Figure 4 shows the change in the value of the panel surface temperature of solar panel with the number of cells.

4. Results and discussion

4.1 Model validation

This study compares the cooling of solar panels using free convection and forced convection for two panel models. The study was conducted throughout the year 2025, using the average day of each month and its average temperature and relative humidity. To ensure accuracy, solar loads were applied that precisely matched the solar irradiance and its direction on the studied day, as well as the studied geographical location. The Figure 5(a,b) illustrates the comparison between the experimental and the simulations results, good agreement is observed between the experimentally measured and numerically simulated temperature values on the surface of the upper plate. It shows that diffuse radiation reaches its maximum around the seventh month, while direct radiation is at its minimum during the same period due to increased atmospheric scattering effects. The panel surface temperature continues to climb between the fifth and ninth months even if the total solar radiation decreases, demonstrating the more significant influence of ambient temperature than radiation intensity.

The graph shows how much sunlight strikes the PV panel each month. The red line represents indirect sunshine; the black squares correspond to direct sunlight; and the black circles relate to full sunlight. The horizontal axis shows chosen dates matching mid-month days all through the year 2025; the left vertical axis shows solar intensity (W/m^2) for direct and total radiation, whereas the right vertical axis shows diffuse radiation intensity. The incident (total) solar radiation shows a somewhat

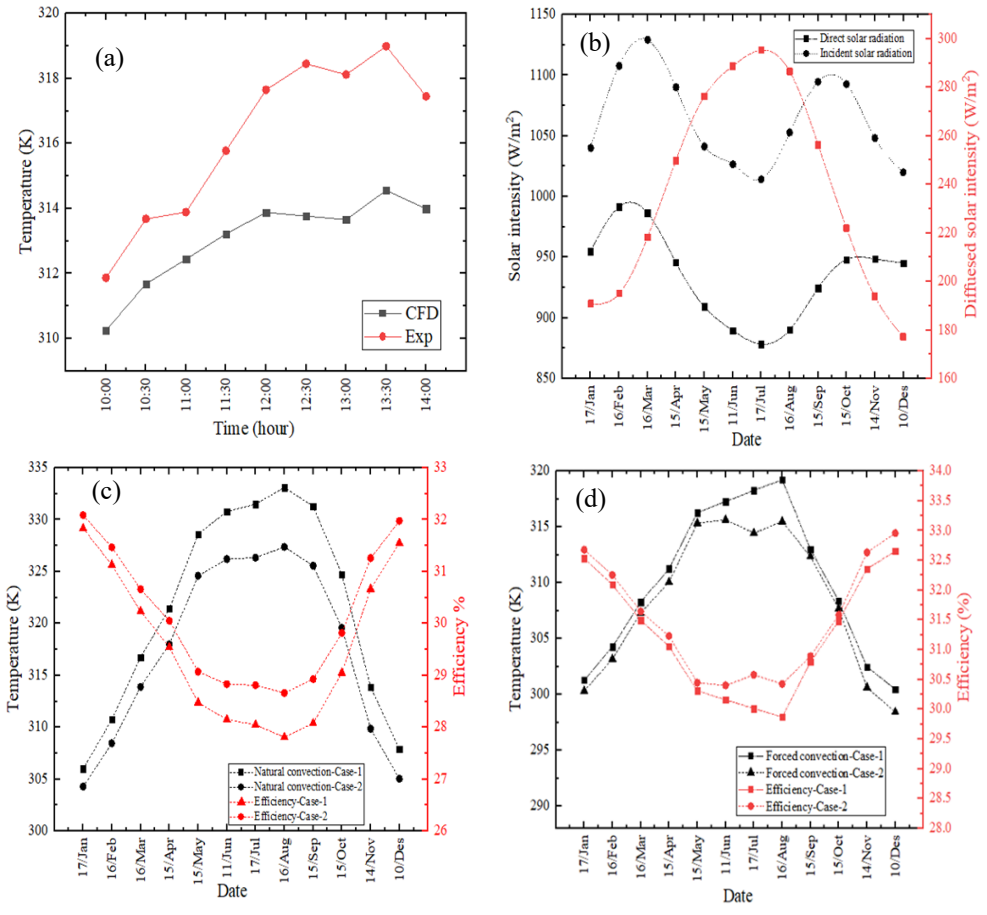

Fig. 5 a) Validation of the experimental and the simulations outcome**, b)** Variation of direct, diffuse, and total solar radiation intensity incident on the photovoltaic panel under representative climatic conditions**, c)** Surface panel temperature and efficiency for natural convection**, d)**Surface panel temperature and efficiency for forced convection

high intensity all year long, with maximum readings happening in March and October, at around 1120-1130 W/m². Therefore, implying atmospheric variables like dust accumulation or increased dispersion, it somewhat decreases in the summer months (June–August). Direct solar radiation exhibits a different pattern, reaching its highest point in late winter and early spring (February-March) before gradually declining to its lowest level in mid-summer (July-August) when values drop below 900 W/m². This drop shows that a lot of solar energy is scattered instead of being absorbed straight away. In contrast, dispersed solar radiation acts in reverst direction to direct radiation. From winter to summer, it climbs steadily, reaching its highest point in July–August (around 300 W/m$_2$) before tapering down as winter approaches. This inverse relationship suggests that atmospheric variables like increased humidity, dust density, and solar elevation cause more scattering in the summer, hence converting more direct radiation into diffuse radiation.

The governing continuity, momentum, species transport and turbulence equation were solver to reproduce the solar panel under natural and forced cooling circumstances. Moreover, for calculating temperature dispassion and heat transmission the energy equation was utilized. The simulation was run under unchanging parameters for each time interval and every variable is discretized second order. The pseudo-transient approach was used to couple pressure and velocity, which increased computing efficiency and ensured stable convergence. The criteria of convergence for the turbulence is fixed at 10^{-4} and for the energy equation increased up to 10^{8} .To confirm the model, the numerical findings of case 1 under natural convection were contrasted with experimental data gathered from a 585 W Jinko solar panel. Sensors positioned on the top surface of the panel were used in testing conducted on November 14 to measure surface temperatures.

Figure 5(c) depicts two scenarios (Case-1 and Case-2) that highlight how the surface panel temperature and efficiency change throughout the year under natural convection. The results suggest that the panel temperature in both cases follows a unique yearly cycle, with lower readings in the winter (January–February and November–December) and higher values in the summer, peaking around July–August in reaction

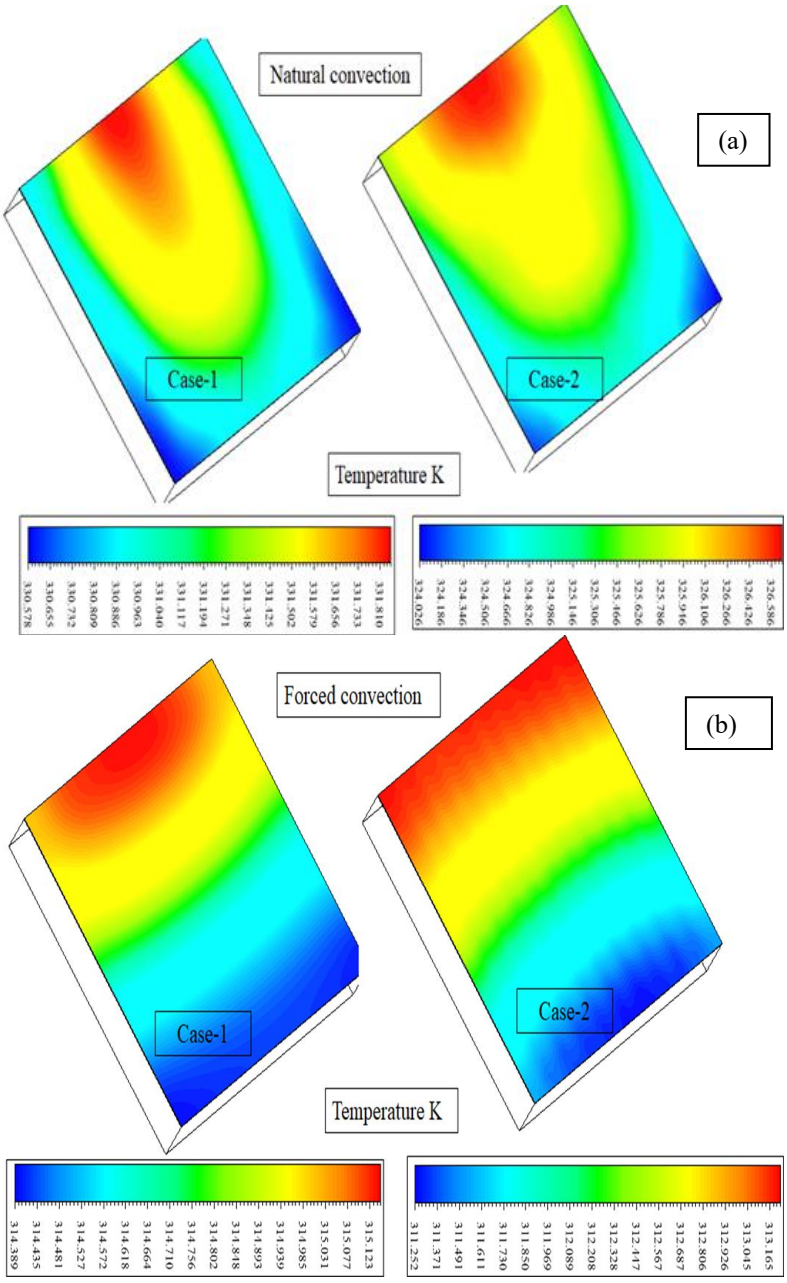

Fig. 6 a) Temperature contours on solar panel under natural cooling, **b)** Temperature contours on solar panel under forced cooling

to increased solar intensity. Case 1's surface temperatures are usually higher than those in Case 2. Conversely, the efficiency shows an opposite pattern with regard to temperature, with greater values found in cooler months (about 31–32%) and lower values throughout warmer months (about 28–29%). All over the year, Case-2 usually attains somewhat greater efficiency than Case-1. This inverse connection emphasizes the negative influence of high temperature on system performance, indicating that better thermal control, as observed in Case-2, helps to increase efficiency, especially during heat surges.

Under forced convection over the year, Figure 5(d) shows the fluctuation of surface panel temperature and efficiency for Case-1 and Case-2. Similar to the natural convection results, the surface temperature in both situations rises from winter to summer, peaks in July-August, and then sinks towards winter. Still, forced airflow's increased heat removal results in noticeably reduced total temperature levels in comparison to natural convection. Case-1 still experiences marginally higher temperatures than Case-2 year-round. The efficiency trends inversely with temperature, meaning that it is higher during cooler months (about 32–33%) and lower during warmer months (about 30-31%). Once again, Case-2 shows somewhat higher efficiency than Case-1. The graph shows that forced convection lowers the panel's operating temperatures by boosting heat regulation, therefore increasing efficiency in comparison to natural convection settings. For forced and free convection cooling under solar radiation. Figure 6(a,b) shows temperature contours. The way the solar panel acts when it is cooled by natural or forced convection is very different in terms of how it transfers heat. Under natural convection, the temperature distribution is very non-uniform, with a clear hot spot focused near the top of the panel. Buoyancy-driven flow causes heated air to rise and build at the top, hence creating thermal stratification. Thus, the lower area stays comparatively colder, while the higher area has higher temperatures, therefore pointing to poor heat transfer and the existence of a thick thermal boundary layer. The hot spot seems more localised in Case-1, but in Case-2 the heat extends somewhat toward the centre, indicating marginally better mixing but still low cooling efficiency.

In contrast, under forced convection as shown in Figure 6(b), the temperature contours become more uniform and smoother due to the presence of externally driven airflow, which enhances convective heat transfer and disrupts the thermal boundary layer. The peak temperature is noticeably reduced, and the high-temperature region is less concentrated compared to natural convection. The isotherms exhibit a gradual and consistent temperature gradient from the top toward the bottom, indicating effective heat removal across the panel surface. Additionally, the cooler regions expand significantly, especially near the lower part of the panel, confirming improved cooling performance. Between the two configurations, Case-2

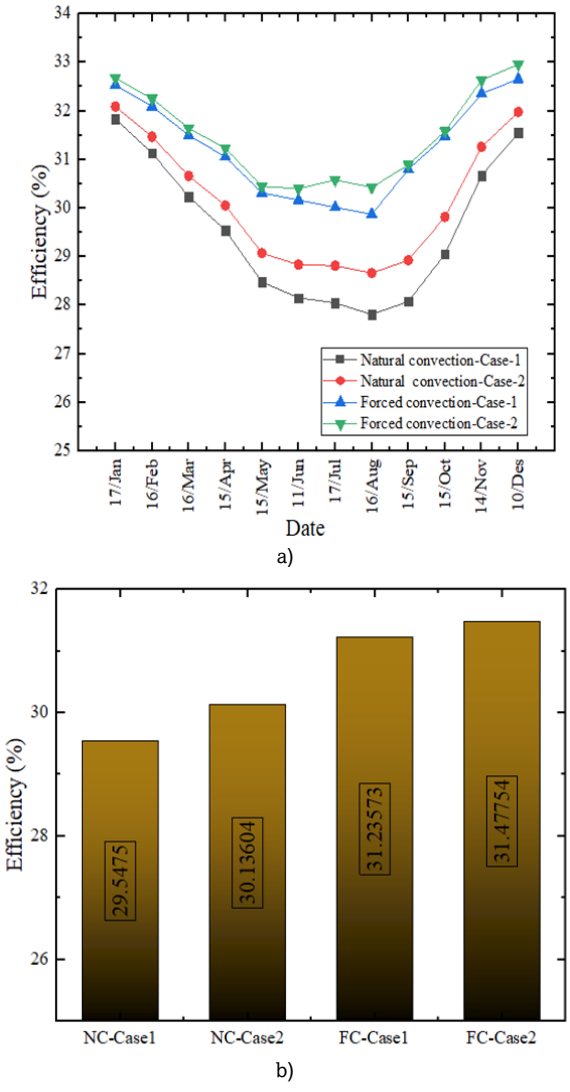

Fig. 7 a) Comparison of the electrical efficiency values of the both models, **b)** Average electrical efficiency over the year

demonstrates a more uniform temperature field than Case-1, implying better flow interaction or design optimization. This result agrees with the findings of Ibrahim *et al.* (2023), who reported that forced convection significantly improves temperature uniformity and reduces the operating temperature of photovoltaic panels compared to natural convection.

The results presented in Figure 7(a,b) align closely with those reported by Hussien *et al.* (2023) concerning the effect of cooling on the performance of PV systems. Both studies show that temperature fluctuations significantly affect PV efficiency; efficiency falls during warmer times and rises under cooler conditions. The clear seasonal pattern seen in Figure 7(a,b) shows that efficiency falls from about 32–33% in the colder months to between 28% and 30% in the warmer months, therefore affirming the inverse connection between temperature and efficiency. Always, forced convection (FC-Case-1 and FC-Case-2) offers greater efficiency than natural convection (NC scenarios); hence, FC matches the findings of Hussien *et al.* (2023), who demonstrated that active cooling improves the performance of PV. Quantitatively, the increase in efficiency in the current findings ranges from roughly 1.1% to 1.9% when comparing forced convection to natural convection, which is somewhat consistent with the reported improvement of up to 2.1% using backside fans and 1.34% using a blower system in the reference study. Moreover, FC-Case-2 has the best efficiency among all designs, therefore implying a more efficient cooling system akin to the fan-based approach determined to be ideal by Hussien *et al.* (2023). The referenced work concentrates on short-term experimental measurements and CFD validation over a single day; the current results provide a wider seasonal view therefore reinforcing the consistency and dependability of forced convection cooling across diverse surroundings.

Figures 8(a) show how air flows over the back of the PV panel, with cooler areas shown in blue and warmer areas moving towards green. This gradient indicates that heat removal is not totally uniform; some areas experience less efficient cooling. The bottom section illustrates a structured network of channels or fin-like structures intended to direct airflow behind the panel. These passageways seek to increase convective heat transmission by increasing surface area and directing air through tiny channels, so increasing velocity and enhancing the heat transfer coefficient. Created cooling systems depending either on forced convection or on a mix of forced airflow and fins normally exhibit such a structure. When compared with the results reported by Ibrahim *et al.* (2025), the Figure 8(b) aligns most closely with the forced-finned PV configuration, which the study identifies as the most effective

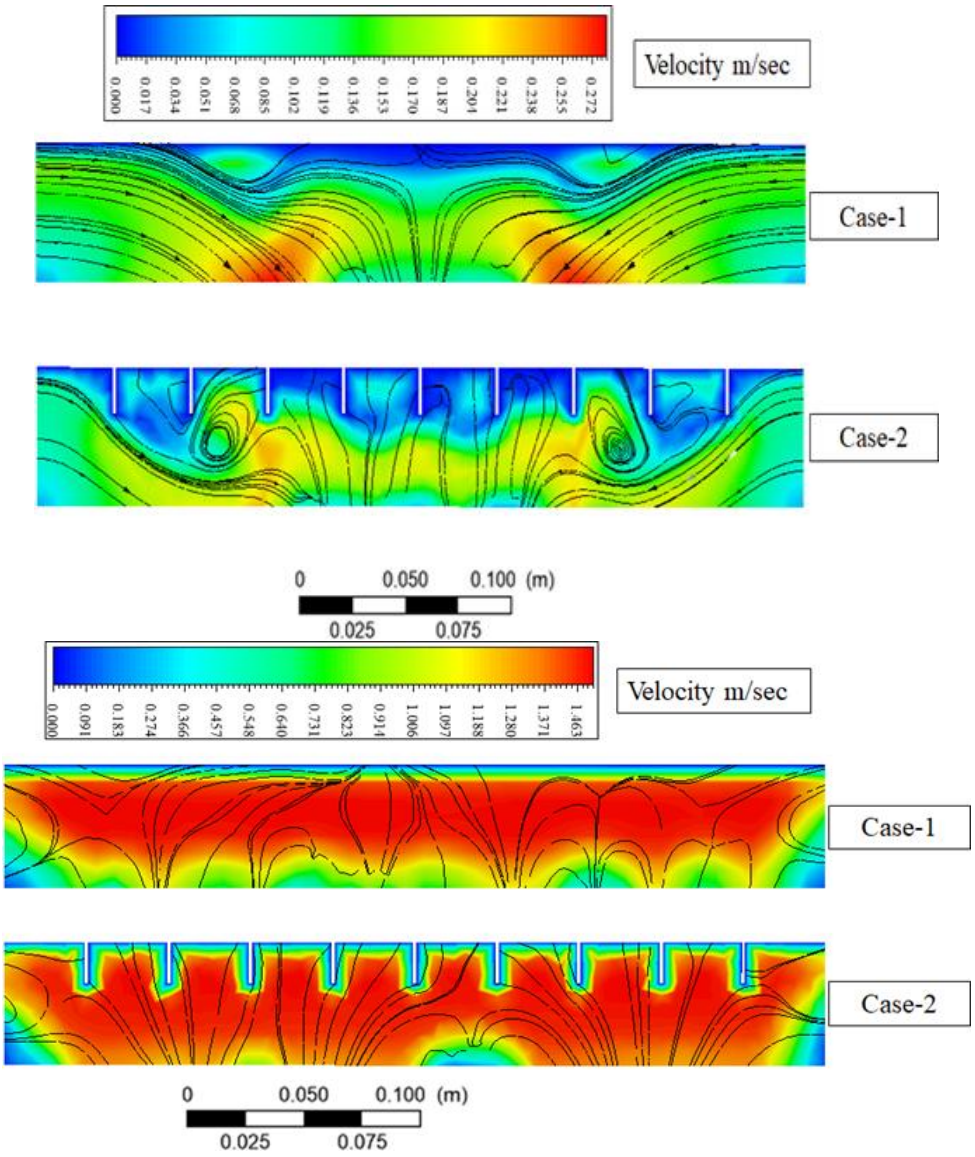

Fig. 8 a) Velocity contours for both models under natural cooling, b) Velocity contours for both models under forced cooling

cooling method among the three evaluated (forced convection PV, free-finned PV, and forced-finned PV). Ibrahim *et al.* (2025) demonstrates that forced-finned systems achieve the highest energy enhancement, savings, and CO_2 emission reductions, reaching 569.09 × R kWh and 330 × R kg CO_2 savings for domestic applications, and significantly larger values at the power plant scale. The visual proof of guided airflow and extended surfaces in the current research supports this result as such designs maximize heat dissipation and so boost the PV electrical efficiency. But the uneven colour distribution in the contour implies that actual systems may experience airflow maldistribution or localized heat buildup, therefore decreasing performance relative to ideal circumstances supposed in parametric studies. Although the forced-finned technique offers the biggest long-term savings, its somewhat longer payback period than simpler forced or passive systems is caused by greater initial complexity and expense. This clarifies why forced cooling's electrical efficiency is comparable across the two models, with the second model exhibiting a small improvement. But in free cooling, the impact of fins is quite evident; just adding fins boosts the electrical efficiency by 2 to 3%. The fins' ability to free cool is better than that of forced cooling, therefore. The fins not only expand the surface area for heat exchange but also generate vortices that raise the convection heat transfer coefficient.

5. Conclusions

This study examined the cooling effectiveness of two distinct types of photovoltaic panels in actual meteorological settings. They studied the average temperature and humidity every month for this and contrasted what occurred with forced and natural convection. This study discovered a major impact on the efficiency of the solar panel due to the heat management and clearly the finned design has advantages. The modified design increased efficiency by approximately 2% under convection, while increases under forced convection climbed to 6.53%. Increasing efficiency by 3.12% boost by forcing the regular panel to cool. Under natural convection in particular, when vortices generated by fins boost heat dissipation, these improvements are primarily attributed to a bigger heat transfer surface area and enhanced convective mixing. The study does have certain constraints, though. The finite-volume model simplifies by assuming steady-state conditions and simple boundary conditions, therefore ignoring possibly transient environmental effects including fluctuating wind, solar radiation changes, and dust buildup. Furthermore, the long-term effect of heat and dampness shows no impact on the materials. The validation is limited to one experimental source, therefore perhaps impacting the extent of generalizability of the findings. Future research should concentrate on transient simulations, more general experimental validation under varied environmental conditions, and the integration of extra real-world factors including dust accumulation and material aging. Financial viability analyses as well as more study on better fin geometries and hybrid cooling methods would help to improve the utility of the work.

Author Contributions: A.A.: Conceptualization, methodology, formal analysis, writing-original draft. M.M.; supervision, resources, Z.A.; writing-review and editing. H.A. & F.A.; writing-review and editing. T.Kh.; Project administration, validation. All authors have read and agreed to the published version of the manuscript.

Conflicts of Interest: The authors declare no conflict of interest.

References

Abbass, O. A., & Abduljabbar, A. A. (2022). Performance of a heat pipe solar collector with evacuated polycarbonate front cover. *Journal of Applied Engineering Science*, 20(3), 852–860. https://doi.org/10.5937/jaes0-33617

Acheme, D. (2025). A Review of Solar Panel Efficiency in Different Weather Condition. *Convergent Materials Horizons*, 1(1), 48-53. https://doi.org/10.64229/fvyzak36

Akpinar, E., Papatya, F., Das, M., Yildirim, S., Alatas, B., Catalkaya, M., & Akay, O. E. (2025). Sustainable Solar Panel Efficiency Optimization with Chaos-Based XAI: An Autonomous Air Conditioning Cabinet-Based Approach. *Sustainability*, 17(16), 7514. https://doi.org/10.3390/su17167514

Ali, H. H. M., Danook, S. H., & Mohiuddin, K. O. (2025). Water Production from Atmospheric Air Using a Solar Water Recuperator by Glass Pyramid Device. *Tikrit Journal of Engineering Sciences*, 32(2), 1-12. https://doi.org/10.25130/tjes.32.2.27

Ali, H. H. M., Hussein, A. M., Allami, K. M. H., & Mohamad, B. (2023). Evaluation of shell and tube heat exchanger performance by using ZnO/water nanofluids. *Journal of Harbin Institute of Technology (New Series)*, 30(6), 62-69, 2023001. https://doi.org/10.11916/j.issn.1005-9113.2023001

Ali, H. H. M., Mohammed, A. J., Alshukri, M. J., Hussien, A. M., & Alsabery, A. I. (2024). Numerical study on entropy minimization in pipes with helical airfoil and CuO nanoparticle integration. *Open Engineering*, 14(1), 20220594. https://doi.org/10.1515/eng-2022-0594

Ali, H.H.M., Ahmed, S.Y. (2024). Assessing the economic viability of solar distillation employing a rotating hollow cylinder. *International Journal of Heat and Technology*, 42(2), 613-619. https://doi.org/10.18280/ijht.420228

Ali, M. H., Mawlood, M. K., & Jalal, R. E. (2024). Performance study of an isolated small scale Trombe wall with partially evacuated air gap. *Advances in Mechanical Engineering*, 16(1), https://doi.org/10.1177/16878132231224996

Avithi Desappan, D., Natarajan, E., & Ponnusamy, L. (2015). Performance evaluation of photovoltaic system in humid atmosphere. *Applied Mechanics and Materials*, 787, 57-61.

Badi, N., & Laatar, A. H. (2024). Improved cooling of photovoltaic panels by natural convection flow in a channel with adiabatic extensions. *Plos one*, 19(7), e0302326. https://doi.org/10.1371/journal.pone.0302326

Barrak, A. S., Ali, N. M., & Ali, H. H. M. (2022). An effect of binary fluid on the thermal performance of pulsation heat pipe. *International Journal of Applied Mechanics and Engineering*, 27(1), 21-34, https://doi.org/10.2478/ijame-2022-0002

Bekbolatova, Z., Grigoryev, D., Minazhova, S., Bekbayev, A., Dauletkhanova, A., & Sarsenbayev, Y. (2025). Advanced computational modelling of photovoltaic module cooling for improved temperature and efficiency profiles. *Engineered Science*, 38, 1984. https://doi.org/10.30919/es1984

Berkache, A., Amroune, S., Golbaf, A., & Mohamad, B. (2022). Experimental and numerical investigations of a turbulent boundary layer under variable temperature gradients. *Journal of the Serbian Society for Computational Mechanics*, 16(1), 1–15. https://doi.org/10.24874/jsscm.2022.16.01.01

Falah Zarda Mohammed, Adnan M. Hussein, Suad H. Danook, Barhm Mohamad; Characterization of a flat plate solar water heating system using different nano-fluids. *AIP Conf. Proc.* 15 December 2023; 2901 (1): 100018. https://doi.org/10.1063/5.0178901

Hasan, D. S., Mansour S. Farhan, & alrikabi, H. (2022). Impact of Cloud, Rain, Humidity, and Wind Velocity on PV Panel Performance. *Wasit Journal of Engineering Sciences*, 10(2), 34-43. https://doi.org/10.31185/ejuow.Vol10.Iss2.237

Hassan, M. K., Alqurashi, I. M., Salama, A. E., & Mohamed, A. F. (2022). Investigation the performance of PV solar cells in extremely hot environments. *Journal of Umm Al-Qura University for Engineering and Architecture*, 13(1), 18-26. https://doi.org/10.1007/s43995-022-00005-x

Homa, M., Sornek, K., & Goryl, W. (2024). Experimental and Numerical Study on Air Cooling System Dedicated to Photovoltaic Panels. *Energies*, 17(16), 3949. https://doi.org/10.3390/en17163949

Hossam, N., Abd El-Hamid, M., Gamal, M., & Fatouh, M. (2025). Thermal management of photovoltaic modules using phase change

materials: Experimental and numerical investigations. *Applied Thermal Engineering*, 279, 127645. https://doi.org/10.1016/j.applthermaleng.2025.127645

Hussien, A., Eltayesh, A., & El-Batsh, H. M. (2023). Experimental and numerical investigation for PV cooling by forced convection. *Alexandria Engineering Journal*, 64, 427–440. https://doi.org/10.1016/j.aej.2022.09.006

Ibrahim, T., Hachem, F., Ramadan, M., Faraj, J., El Achkar, G., & Khaled, M. (2023). Cooling PV panels by free and forced convections: Experiments and comparative study. *AIMS Energy*, 11(5), 774–794. https://doi.org/10.3934/energy.2023038

Ibrahim, T., Faraj, J., Kisswani, K., El Achkar, G., Murr, R., & Khaled, M. (2025). Cooling photovoltaic panels with air convection: Parametric environmental and economic analysis with case studies. e-Prime - Advances in Electrical Engineering, *Electronics and Energy*, 12, 101020. https://doi.org/10.1016/j.prime.2025.101020

Khodadadi, M., & Sheikholeslami, M. (2022). Assessment of photovoltaic thermal unit equipped with phase change material in different finned containers. *Journal of Energy Storage*, 46, 103939. https://doi.org/10.1016/j.est.2021.103939

Kumar, S., & Subbarao, P. M. V. (2025). Investigation of convective cooling characteristics and thermal profiling of a free-standing solar photovoltaic system. *Thermal Science and Engineering Progress, 65*, 103950. https://doi.org/10.1016/j.tsep.2025.103950

Manar, M., Jafari, M., Ranjbar, F., & Garousi Farshi, L. (2025). Assessing the impact of cavity structure on collector and using PCMs on solar chimney power plant performance. *International Journal of Heat and Technology*, 43(2), 721-730, https://doi.org/10.18280/ijht.430231

Miri, R., Mliki , B., Mohamad, B. A., Abbassi, M. A., Mowffaq Oreijah, Kamel Guedri, & Abderafi, S. (2023). Entropy generation and heat transfer rate for MHD forced convection of nanoliquid in presence of viscous dissipation term. CFD *Letters*, 15(12), 77–106. https://doi.org/10.37934/cfdl.15.12.77106

Mohamad, B. (2024). Improving Heat Transfer Performance of Flat Plate Water Solar Collectors Using Nanofluids. *Journal of Harbin Institute of Technology (New Series)*, 32(2):80-89. https://doi.org/10.11916/j.issn.1005-9113.2024001

Mohanty, C. P., Behura, A. K., Singh, M. R., Prasad, B. N., Kumar, A., Dwivedi, G., & Verma, P. (2024). Parametric performance optimization of three sides roughened solar air heater. *Energy Sources, Part A: Recovery, Utilization and Environmental Effects*, 46(1), 7214-7234. https://doi.org/10.1080/15567036.2020.1752855

NematpourKeshteli, A., Iasiello, M., Langella, G., & Bianco, N. (2024). Using metal foam and nanoparticle additives with different fin shapes for PCM-based thermal storage in flat plate solar collectors. *Thermal Science and Engineering Progress*, 52, 102690. https://doi.org/10.1016/j.tsep.2024.102690

Omri, M., Selimefendigil, F., Smaoui, H. T., & Kolsi, L. (2022). Cooling system design for photovoltaic thermal management by using multiple porous deflectors and nanofluid. *Case Studies in Thermal Engineering*, 39, 102405. https://doi.org/10.1016/j.csite.2022.102405

Qader, F. F., Mohamad, B., Hussein, A. M., & Danook, S. H. (2024). Numerical study of heat transfer in circular pipe filled with porous medium. *Pollack Periodica*, 19(1), 137-142. https://doi.org/10.1556/606.2023.00869

Qader, F. F., Mohammed, F. Z., & Mohamad, B. (2024). Thermodynamic analysis and optimization of flat plate solar collector using TiO_2/water nanofluid. *Journal of Harbin Institute of Technology (New Series)*, 31(4), 61–73. https://doi.org/10.11916/j.issn.1005-9113.2023050

Qader, F., Hussein, A., Danook, S., Mohamad, B., & Khaleel, O. (2023). Enhancement of double-pipe heat exchanger effectiveness by using porous media and TiO_2 water. *CFD Letters*, 15(4), 31–42. https://doi.org/10.37934/cfdl.15.4.3142

Raza, S., Farooq, A., Shehzad, M. S., Hussain, W., Abbas, Z., & Im, I.-T. (2026). A CFD analysis of photovoltaic panel cooling: A review. *International Journal of Air-Conditioning and Refrigeration*, 34(1), 2. https://doi.org/10.1007/s44189-025-00096-w

Sardouei, M. M., Mortezapour, H., & Jafari Naeimi, K. (2018). Temperature distribution and efficiency assessment of different PVT water collector designs. *Sādhanā*, 43(6), 84. https://doi.org/10.1007/s12046-018-0826-x

Sepúlveda-Oviedo, E. H. (2025). Impact of environmental factors on photovoltaic system performance degradation. *Energy Strategy Reviews*, 59, 101682. https://doi.org/10.1016/j.esr.2025.101682

Seto, D., Arifin, Z., Kristiawan, B., & Prasetyo, S. (2024). Nanoparticle-enhanced phase change materials (NePCM) in passive cooling systems to improve solar panel efficiency. *International Review of Mechanical Engineering (IREME)*, 18(1). https://doi.org/10.15866/ireme.v18i1.24149

Sheikh, Y., Jasim, M., Qasim, M., Qaisieh, A., Hamdan, M. O., & Abed, F. (2024). Enhancing PV solar panel efficiency through integration with a passive multi-layered PCMs cooling system: A numerical study. *International Journal of Thermofluids*, 23, 100748. https://doi.org/10.1016/j.ijft.2024.100748

Shrivastava, A., Prakash Arul Jose, J., Borole, Y. D., Saravanakumar, R., Sharifpur, M., Harasi, H., Abdul Razak, R. K., & Afzal, A. (2022). A study on the effects of forced air-cooling enhancements on a 150 W solar photovoltaic thermal collector for green cities. *Sustainable Energy Technologies and Assessments*, 49, 101782. https://doi.org/10.1016/j.seta.2021.101782

Sun, J., He, Y., Li, X., Lu, Z., & Yang, X. (2023). CFD simulations for layout optimal design for ground-mounted photovoltaic panel arrays. , 105558. https://doi.org/10.1016/j.jweia.2023.105558

Tripathi, A. K., Ray, S., Aruna, M., & Prasad, S. (2021). Evaluation of solar PV panel performance under humid atmosphere. *Materials Today: Proceedings*, 45, 5916-5920. https://doi.org/10.1016/j.matpr.2020.08.775

Wen, Y., Li, X., Hu, W., Yang, F., Yang, K., & Wang, J. (2025). Experimental research on the temperature distribution characteristics of photovoltaic array. *Applied Thermal Engineering*, 265, 125507. https://doi.org/10.1016/j.applthermaleng.2025.125507

Zarda, F., Hussein, A., Danook, S., & Mohamad, B. (2022). Enhancement of thermal efficiency of nanofluid flows in a flat solar collector using CFD. *Diagnostyka*, 23(4), 1–9. https://doi.org/10.29354/diag/156384

Zina Abd Alameer Al Shadidi. (2020). The Effect of Environmental Factors (Temperatures & Humidity) on the Solar Cell Performance / Matlab Model. *International Journal of Applied Mathematics and Theoretical Physics*, 6(4), 61-67. https://doi.org/10.11648/j.ijamtp.20200604.12